Available online at www.sciencedirect.com
ScienceDirect
Physica E 38 (2007) 128–134
PHYSICA E
www.elsevier.com/locate/physe

Quantum confinement and interface structure of Si nanocrystals of sizes 3–5 nm embedded in a-SiO_2

Emmanouil Lioudakis[a,*], Andreas Othonos[a], G.C. Hadjisavvas[b], P.C. Kelires[b], A.G. Nassiopoulou[c]

[a]*Department of Physics, Research Center of Ultrafast Science, University of Cyprus, P.O. Box 20537, Nicosia 1678, Cyprus*
[b]*Physics Department, University of Crete, P.O. Box 2208, 710 03 Heraclion, Crete, Greece*
[c]*IMEL/NCSR Demokritos, P.O. Box 60228, 15310 Aghia Paraskevi, Athens, Greece*

Available online 16 December 2006

Abstract

Spectroscopic ellipsometry and Monte Carlo simulations are employed to answer the fundamental question whether the energy gaps of Si nanocrystals with sizes in the range of 3–5 nm, which are embedded in amorphous silica, follow or deviate from the quantum confinement model, and to examine their interfacial structure. It is shown that the optical properties of these nanocrystals are well described by the Forouhi–Bloomer interband model. Analysis of the optical measurements over a photon-energy range of 1.5–5 eV shows that the gap of embedded nanocrystals with a mean size of ~3.9 nm follows closely quantum confinement theory. A large band gap expansion (~0.65 eV) compared to bulk Si is observed. The Monte Carlo simulations reveal a non-abrupt interface and a large fraction of interface oxygen bonds. This, in conjunction with the experimental observations, indicates that oxygen states and the chemical disorder at the interface have a negligible influence on the optical properties of the material in this size regime.

PACS: 78.67.−n; 78.67.Bf

Keywords: Monte Carlo simulations; Silicon nanocrystals; Spectroscopic ellipsometry; Optical properties

1. Introduction

Silicon nanocrystals (Si-NCs) embedded in silicon dioxide (a-SiO_2) matrix have been extensively studied in recent years, both for their fundamental properties [1–3] and their potential applications in photonics and nanoelectronics [4–8]. Fundamental interest focuses on the origin of light emission and on band gap expansion as the NC size shrinks. As in the similar case of porous Si (p-Si) [3,9], the interpretation of these phenomena relies on models based on the interplay between quantum confinement (QC) effects [1,2], which tend to open up the gap, and oxygen-related localized surface states [3,10,11], which tend to pin the gap.

The separation of these two effects and the estimation of their relative contribution to the gap size remains a challenge. In the case of p-Si, Wolkin et al. [3] have convincingly shown that for Si-NC sizes slightly larger than ~3 nm the experimentally deduced PL energies, and the associated gaps, coincide with QC theory, which indicates free excitonic recombination and independence from surface bonds. For sizes less than 3 nm, localized states due to oxygen bonds at the surface were shown to drastically lower the gap from the QC value.

This information is also relevant to the Si-NC/a-SiO_2 case. Oxygen states at the interface of small Si-NCs are believed to contribute to the pinning of the gap from QC values [12–14]. In addition, contributions from inner core NC structural deformations were also suggested [15] as possible sources of the pinning. However, the effect in this size regime, below 3 nm, is far from being well understood. On the other hand, in the size regime over 3 nm, especially in the critical transition region between 3 and 5 nm where a vast fraction of Si-NCs is usually found, the picture derived from experimental measurements is rather vague.

*Corresponding author. Tel./fax: +357 22892821.
E-mail address: mlioud@ucy.ac.cy (E. Lioudakis).

1386-9477/$ - see front matter © 2007 Elsevier B.V. All rights reserved.
doi:10.1016/j.physe.2006.12.020

The central question is whether the gap and PL energies follow the QC theory [1,2], which would indicate free excitonic recombination as the source of radiative emission, like the case of p-Si [3], or whether the energies significantly deviate from QC values, which would indicate that interface oxygen states play a significant role in the optical activity of the material. Some studies [13,16] extracted gap values close to what is predicted by QC theory, though they proposed that the dominant emission is related to a fundamental transition spatially located at the interface. However, other studies [12,17] extracted gap values deviating from (lower than) QC theory, suggesting that interface states still play a role in this size regime. It has even been suggested [18,19] that interface states dominate the QC effect.

The clarification of this fundamental point is crucial for the optimization, design, and successful implementation of this material in optoelectronic devices. The Si-NC/a-SiO_2 system is superior to p-Si with respect to stability, and the a-SiO_2 matrix provides excellent chemical and electrical passivation of the NCs. Recently, a lot of experimental work using spectroscopic ellipsometry (SE) has been reported to investigate the depth profiling of the Si-NCs in Si-implanted SiO_2 films [20,21] as well as the size effect of NCs by the rapid thermal annealing [22].

In this paper, we report on the results of SE measurements, supplemented by Monte Carlo (MC) simulations of the interface structure, which clearly demonstrate that the gap energies of Si-NC/a-SiO_2 with sizes in the range of 3–5 nm closely follow the QC theory, in agreement with the results of Wolkin et al. [3] for p-Si. Our experimental analysis depicts a large band gap expansion ($\sim$0.65 eV) and a significant reduction in the optical constants (ε_1 and ε_2) as compared with that of crystalline bulk silicon. The change in spectrum shape of optical dielectric functions may be attributed to the shift of transition energies and redistribution of oscillator strength caused by the quantum size effect. Furthermore, the MC simulations find a non-abrupt interface, rich in suboxide components, and a large fraction of Si–O–Si bridge bonds, which were shown to lead to gap reductions in isolated small NC [11]. Thus, despite the abundance of such oxygen bonds at the interface, their influence on the optoelectronic properties of NCs with sizes in the range of 3–5 nm seems to be negligible.

The paper is organized as follows. In the following section, we describe the methodologies on which the optical measurements and the simulations are based. We also describe the technical details of the growth method and the macroscopic structural characteristics of the Si-NCs. Section 3 presents the results and the accompanying discussion. Finally, Section 4 gives our conclusions.

2. Methodology

SE has been established to be a very effective optical characterization technique of semiconductor samples with very high sensitivity and accuracy [23]. The ellipsometer consists of a broadband light source followed by a polarizer and a retarder, which are attached to the incoming section. The polarized broadband light is then incident to the sample and the reflected beam, after passing through an analyzer, enters a monochromator in order to select the spectrum region of interest. Light intensity is measured by a detector, which is placed after the monochromator. The ellipsometer is an instrument that allows full characterization of the optical properties of thin films [24]. Using the ellipsometric parameters $\tan\Psi$ and $\cos\Delta$ [25], where Ψ and Δ are the ellipsometric angles that describe the reflection of the polarized light, the thickness and the dielectric functions of the Si-NC sample can be determined using an appropriate optical/structural model.

Furthermore, in order to analyze the dielectric functions of Si-NCs, a Forouhi–Bloomer (FB) interband model is used [26]. In this model, the extinction coefficient is given by

$$k(E) = \left[\sum_{i=1}^{3} \frac{A_i}{E^2 - B_i E + C_i}\right](E - E_g)^2$$

and the refractive index determined from Kramers–Kronig analysis is given by

$$n(E) = n_\infty + \sum_{i=1}^{3} \frac{B_{0_i} E + C_{0_i}}{E^2 - B_i E + C_i},$$

where

$$B_{0_i} = \frac{A_i}{Q_i}\left[-\frac{B_i^2}{2} + E_g B_i - E_g^2 + C_i\right],$$

$$C_{0_i} = \frac{A_i}{Q_i}\left[(E_g^2 + C_i)\frac{B_i}{2} - 2E_g C_i\right],$$

$$Q_i = \frac{1}{2}(4C_i - B_i^2)^{1/2},$$

where A_i, B_i and C_i ($i = 1$, 2, and 3) are some parameters related to electron transition, n_∞ is the refractive index when the photon energy $E \to \infty$, and E_g is the energy band gap of the Si-NCs. We note that an approximate value for A_i can be obtained by the knowledge of the magnitude of the peaks. The initial guess for n_∞ was chosen as unity. In the spectral fitting, the optimization procedure was carried out by freely varying the parameters to minimize a mean-square error.

Si-NCs within SiO_2 are formed by low-pressure chemical vapor deposition (LPCVD) of amorphous silicon on a thin tunneling thermal oxide ($\sim$3.5 nm), followed by high temperature oxidation (900 °C, 20 min) and annealing (900 °C, 1 h). The silicon substrate is an n-type wafer with resistivity in the range of 1–2 Ω cm. The resulting structure is composed of Si-NCs with size of 3.9 nm in the z-direction and slightly larger in the x–y directions, embedded within two silicon oxide films:

a bottom tunneling oxide, 3.5 nm thick, and a top oxide (resulting from the oxidation of the deposited silicon layer), ~9.5 nm thick. More details on the fabrication and characterization of the NCs are given elsewhere [8]. The advantage of this fabrication technique is that the vertical size of the dots is controlled with accuracy by controlling the deposited amorphous layer thickness and the oxidation time. The tunnel silicon oxide layer is pre-fabricated before dot growth and it is not affected by the next processing steps. The interfaces between the NCs and the tunnel and top oxides are quite sharp. Previous reports demonstrated that this method of synthesis of Si-NCs within SiO_2 constitutes a single and reliable process for the fabrication of silicon nanocrystal memory devices [27].

For the simulation of the structure of the embedded Si-NCs, which is especially complicated at the interface with the oxide, we employ a MC methodology that has been well tested and applied with success for the description of NCs with smaller sizes [15], where deformations and distortions become crucial, as well as for the description of the planar interface [28]. In this method, the Si/a-SiO_2 system is modeled as a defect-free network in which Si and O have four and two bonds, respectively, without any O–O bonds. The energy is approximated by a Keating-like valence force model. This is composed of two terms representing the cost for bond-length and bond-angle distortions (strain energy), and an additional "suboxide penalty" term, which takes into account the chemical energy cost for the formation of suboxides [29]. The details about the functional form and parameters of the model can be found in Ref. [29].

The host amorphous oxide matrix is generated by using the well-known MC algorithm of Wooten et al. [30]. One forms a continuous random network starting from the perfect crystal, beta-crystobalite in this case, by bond breaking and switching moves [28,30]. To compositionally equilibrate the interface, we have introduced [15] bond conversion moves, which exchange a Si–Si bond in the NCs with a neighboring Si–O–Si bond in the oxide. In both types of moves, we first relax locally the structure, following the attempted move, using a steepest-descent method minimizing the forces on the atoms. Then, the change in energy between this final and the initial configuration is calculated. The attempted move is accepted or rejected according to the Metropolis criterion. Details about the generation of the composite system (NCs plus oxide) can be found in Ref. [15]. In the final stage, the fully relaxed and equilibrated structure contains NCs with a size of 4 nm, to realistically simulate our experimental sample, which contains NCs with a mean size of 3.9 nm. The number of atoms in the NC is ~1700. The whole structure contains ~14,100 atoms. The total content of Si in the composite structure is 41%. The cell is subjected to periodic boundary conditions in all directions.

3. Results and discussion

3.1. Ellipsometric results and analysis

Here, we performed ex situ ellipsometric measurements in a Si-NCs sample using a multiwavelength spectroscopic ellipsometer (type GES5-SOPRA). Our thin Si-NCs region is represented using Bruggeman effective medium approximation (BEMA) [31] and the obtained dielectric functions are analyzed by the FB model. Fig. 1 shows both ellipsometric parameters for the Si-NCs and bulk silicon reference (c-Si) sample as a function of wavelength in the spectral region of 250–900 nm with steps of 10 nm at an incident optimum angle of 75°. As seen from the above figure, the ellipsometric measurements of Si-NCs sample are different from that of bulk c-Si. The $\tan\Psi$ data of NCs is shifted in higher values and the $\cos\Delta$ data present a different spectral behavior, starting with an observed shift in higher values for small wavelength and a reduction in smaller values from that of c-Si for long wavelength.

In order to investigate the optical properties of Si-NCs sample we have used an optical/structural model to fit the experimental data obtained from the ellipsometry. The structural model that we have adapted for our sample consists of the silicon substrate, one mixture layer (4.9 nm thick) containing the Si-NCs, and a top silicon oxide layer (13.8 nm thick). The embedded NCs in the above model are represented using BEMA mixture of SiO_2 and grained polycrystalline silicon (poly-Si) [32]. The model is then self-consistent and the two involved media play exactly the same role. The effective dielectric functions of this thin NCs region (~4.9 nm) is given by the second-order equation:

$$0 = f\frac{\varepsilon_1 - \varepsilon_{\text{Si-NC}}}{\varepsilon_1 + 2\varepsilon_{\text{Si-NC}}} + (1-f)\frac{\varepsilon_2 - \varepsilon_{\text{Si-NC}}}{\varepsilon_2 + 2\varepsilon_{\text{Si-NC}}},$$

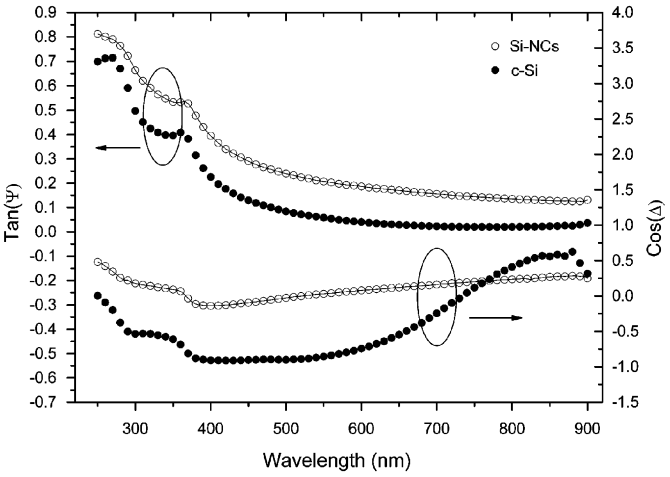

Fig. 1. Ellipsometric parameters for Si-NCs and bulk silicon reference sample as a function of wavelength. The lines represent the best fit with the approach described in the text.

where ε_1 and ε_2 are the dielectric functions of SiO_2 and grained poly-Si, respectively and f is the volume ratio of poly-Si to SiO_2 matrix. We note that the above thicknesses as well as the concentration of poly-Si in SiO_2 ($f = 0.8$) were determined using a nonlinear Levenberg–Marquardt regression method and the regression curves are depicted by the solid lines throughout the experimental data in Fig. 1. The calculated size (3.9 nm) of NCs, obtained from the BEMA mixture, is in excellent agreement with the size of NCs obtained by transmission electron microscopy (TEM). The thickness of this region provides that our sample has almost one monolayer of Si-NCs in host material SiO_2. The obtained effective dielectric function $\varepsilon_{\text{Si-NC}}$ of embedded NCs in host matrix as a function of the energy (1.5–5 eV) is shown in Fig. 2. We observed a significant reduction and a shift of the transition energy peaks in the optical dielectric functions of Si-NCs compared with that of c-Si. We note a change of the absorption edge, which appeared in the imaginary part of dielectric function between two materials.

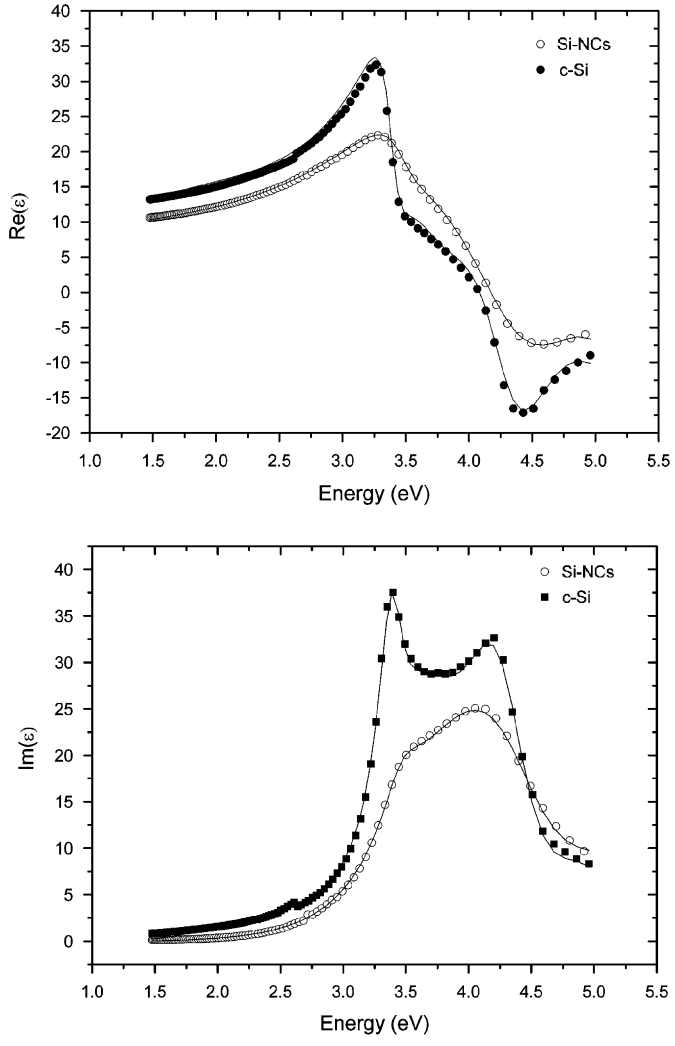

Fig. 2. Dielectric functions of embedded (3.9 nm) Si-NCs in SiO_2 matrix and c-Si sample as a function of energy.

Employing a three-term FB interband model we are able to investigate the energy band gap and the critical points (transition energies) of the Si-NCs region. The model is the most suitable for yielding a successful fitting over the energy range (see the solid lines throughout the dielectric functions data). We have applied this model to both Si-NCs and c-Si reference samples. The position of the ith peak in the extinction coefficient spectrum is given by

$$B_i \approx 2E_i^{\text{peak}},$$
$$C_i \approx (E_i^{\text{peak}})^2.$$

The extracted energy band gap and the critical points E_1, E_2 and E_3 in the Si-NCs region and the reference sample are given in Table 1. The critical point E_1, E_2 observed between 3.0 and 3.7 eV in the spectra is attributed to two kinds of transition. The first corresponds to transitions taking place along the Λ directions of the Brillouin zone, and the second is the lowest direct energy gap located at the Γ point. The critical point between 4.0 and 4.5 eV is labeled E_3, and is attributed to several transitions in the band. Their origin in the Brillouin zone is not well defined, and they are usually attributed to the area including or near the X and Σ points in k space. The theoretical plots of the dielectric functions in Fig. 2 were calculated by using the relations $\varepsilon_1 = n^2 - k^2$ and $\varepsilon_2 = 2nk$, respectively. We should point out that the critical points of c-Si are very close to the values of literature [33]. The results for the Si-NCs region indicate a large band gap expansion (~0.65 eV) and a small shift of transition energies from that of c-Si. Furthermore, as seen from the above results the Si-NCs transition energies in Brillouin zone present different spectral behavior since they are shifted in different sides of the energy range. Similar behavior has been observed using PL excitation technique by Ben-Chorin et al. [34] in porous silicon. We believe that the reduction in the dielectric functions (see Fig. 2) and the observed blue shift at critical transitions are attributed to the energy gap expansion of the Si-NCs and to a redistribution of oscillator strength as a result of QC.

The central finding of our analysis is that the observed band gap expansion is in excellent agreement with what is predicted by QC theory. Indeed, the extracted gap (1.7 eV) nearly coincides with the theoretical gaps calculated using the tight-binding method in Ref. [2] and the empirical pseudopotential method in Ref. [1] at NCs size of 3.9 nm. Furthermore, the extracted results from the FB model yield:

$$\Delta E = E_{\text{g}} - E_{\text{go}} = \frac{a}{d^n},$$

where d is the NC size in nm, E_{g} is the band gap of the Si-NC in eV, E_{go} is the band gap of bulk c-Si, $a = 3.9$ and $n = 1.305$.

The coincidence of our experimental gap with the prediction of QC theory indicates that oxygen-related interface states, which are competitive to QC in influencing

the gap, either are absent or do not affect the optical properties in this size regime. We clarify this issue in the following section.

3.2. MC simulations

In order to shed some light into the above question, we analyze here the atomistic interfacial structure of the Si-NCs/a-SiO_2 nanocomposite system, generated and equilibrated by MC simulations as described in Section 2.

A thin slice cut of the simulational cell is shown in Fig. 3(a). The NC size (diameter) is 4 nm. It is obvious that the distortions induced on the NC due to the embedding in the oxide matrix are small at this size, and are solely concentrated at the interface. The notable finding of our close inspection of the interface is that a considerable number of Si–O–Si bridge bonds, in which an O atom connects two Si atoms terminating the Si-NC, have been formed at the interface. Their relative fraction, with respect to the total number of interface bonds, is about 65%. (The other type of bond is the regular Si–O–Si bond, where an O atom connects a Si atom of the NC with a Si atom in the oxide.) The driving force for their formation is the lowering of the interfacial strain energy [15,28,35] because they can be stretched and bent with minimal energy cost.

Table 1
Critical points of energy transitions and energy band gap of Si-NCs region and reference c-Si sample

Sample	E_g (eV)	E_1 (eV)	E_2 (eV)	E_3 (eV)
c-Si	1.040	3.395	3.640	4.315
Si-NCs	1.700	3.465	3.575	4.325
ΔE (eV)	−0.660	−0.070	0.065	−0.010

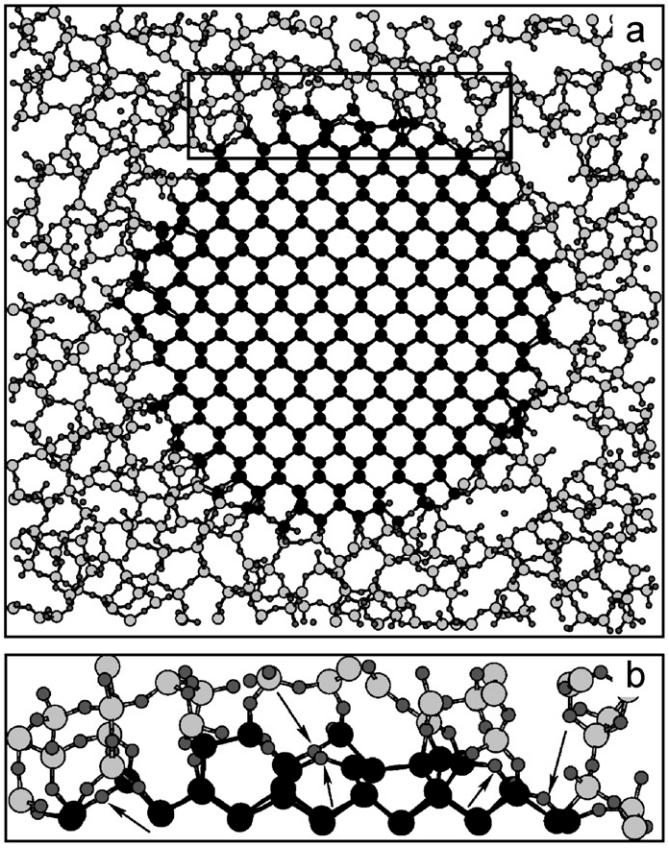

Fig. 3. (a) Ball and stick model of a thin slice cut of a Si-NC embedded in a-SiO_2. (b) Part of the interface magnified. Dark spheres show Si atoms in the nanocrystal. Large (small) gray spheres denote Si (O) atoms in the oxide, respectively. Arrows in (b) indicate the formation of bridge bonds.

The other crucial issue to examine is the abruptness of the interface and its chemical disorder. For this purpose, we need to specify the nominal position of the spherical interface. This is provided by the mean suboxide distance $\bar{r}$, defined [28] by $\bar{r} = \sum r_i / N_{sub}$, where N_{sub} is the number of Si suboxide atoms and r_i is the distance of suboxide atom i from the center of the nanocrystal. In the present case the nominal position of the interface is found to be ~2.0 nm. We then calculate the distributions of suboxide components in both sides of this nominal position. The term "suboxide" indicates the oxidation state, i.e., the number of oxygen first nearest-neighbour atoms, of Si atoms in the network, other than +4 (a Si atom deep in the oxide) and +0 (a Si atom in the core of the NC).

The suboxide distributions are shown in Fig. 4. The vertical line represents the nominal position of the interface. It is clear that we have a coexistence of suboxide components over a wide range, which reveals a non-abrupt transition interfacial layer with a width of ~0.8 nm. We should point out that similar results have been shown by ab initio calculations from embedded Si-NCs [36]. In more detail, we see that Si^{+1} is found toward the Si-NC, Si^{+3} occurs mainly toward the oxide, while Si^{+2} is equally concentrated in both sides of the interface, as the peak is close to the nominal position.

Summarizing, our atomistic analysis of the interface structure reveals that a large fraction of oxygen bridge

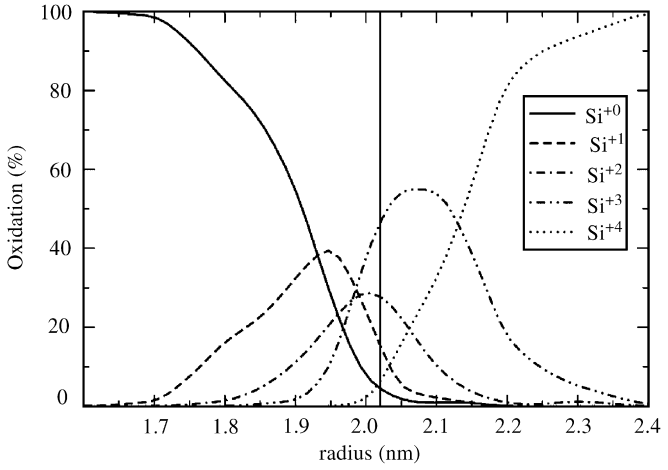

Fig. 4. Oxidation number vs. the distance from the center of the nanocrystal. The vertical solid line shows the nominal position of the interface.

bonds and considerable chemical disorder exist at the interface. Bridge bonds were shown to lead to significant gap reductions in isolated small NCs [11]. Therefore, if this was also true for the embedded NCs, one would expect that the presence of a large fraction of such bonds should pin the gap from the QC value, and point to a stronger role of interface state recombination effects, compared to a weaker role of QC effects. Nevertheless, our experimental results suggest that despite the abundance of bridge bonds and the considerable non-abruptness and chemical disorder at the interface neither the first nor the latter factor play such a significant role at this size regime over 3 nm. The QC effect clearly dominates the emission process. However, we cannot exclude the possibility that some recombination events are spatially located at the interface with the assistance of local Si-O vibrations, as suggested in Ref. [16]. Our results are in accord with the conclusions reached by Wolkin et al. [3] for p-Si in the size regime over 3 nm.

Unfortunately, due to the huge size of the simulational cell, which has to have realistic dimensions, we cannot calculate the electronic structure and the optical properties of our composite structure. However, we are in the process of doing so [37] for smaller NCs in order to answer to the equally important question whether the experimentally verified by many researchers pinning of the gap is due to the oxygen states alone, or in part due to the significant disorder and deformations in the embedded small NCs [15].

4. Conclusions

In conclusion, we have answered the fundamental question whether the energy gaps of large Si-NCs, in the size regime over 3 nm, which are embedded in amorphous silica, follow or deviate from the QC model, and we have examined their interfacial structure. An energy gap of about 1.7 eV for embedded Si-NCs (~3.9 nm) in a-SiO_2 is found, which is analogous to the finding for p-Si in the region, where PL is due to free excitons. We have found that the large fraction of bridge bonds (65%) and the transition layer (~0.8 nm) of the interface have negligible influence in the optical properties (dielectric functions) of these systems. The experimental and theoretical results reveal a verification of QC for thin Si-NCs region providing dynamic information about the optical properties and the electronic band-structure of this material. In addition, this work demonstrates the importance of SE in determining non-destructively the dielectric functions in nanostructures that have potential applications in optoelectronic devices [7]. Finally, we should point out that SE reveals information regarding ground state properties (related to absorption) as opposed to most other reported experimental techniques, which give information related to excited states.

Acknowledgments

This work is supported by a Greece–Cyprus bilateral Grant (ΕΠΑΝ M. 4.3.6.1 and ΚΥ-ΕΛ/0603/67) from the General Secretariat for Research and Technology of Greece and Cyprus Research Promotion Foundation, a grant from the EU and the Ministry of National Education and Religious Affairs of Greece through the action "ΕΠΕΑΕΚ" (program "ΗΡΑΚΛΕΙΤΟΣ") and by a grant from Leventis Foundation Research Committee (program "PULSE") in Cyprus.

References

[1] L.W. Wang, A. Zunger, J. Phys. Chem. 98 (1994) 2158.
[2] J.P. Proot, C. Delerue, G. Allan, Appl. Phys. Lett. 61 (1992) 1948; C. Delerue, G. Allan, M. Lannoo, Phys. Rev. B 48 (1993) 11024.
[3] M.V. Wolkin, J. Jorne, P.M. Fauchet, G. Allan, C. Delerue, Phys. Rev. Lett. 82 (1999) 197.
[4] P. Photopoulos, A.G. Nassiopoulou, D.N. Kouvatsos, A. Travlos, Appl. Phys. Lett 76 (2000) 3588.
[5] A.G. Nassiopoulou, H.S. Nalwa (Eds.), Encyclopedia of Nanoscience and Nanotechnology, vol. 9, American Scientific Publishers, California, 2004, pp. 793–813.
[6] L. Pavesi, L. Dal Negro, C. Mazzoleni, G. Franzo, F. Priolo, Nature (London) 408 (2000) 440.
[7] A.G. Nassiopoulou, A. Solonidou, A. Olzierski, M. Kokonou, E. Tsoi, P. Normand, K. Giannakopoulos, in: Proceedings of the First International Workshop on Semiconductor Nanocrystals, SEMINANO 2005, held in Budapest, vol. 2, 2005, pp. 405–410.
[8] A. Salonidou, A.G. Nassiopoulou, A. Travlos, V. Ioannou-Sougleridis, E. Tsoi, Nanotechnology 15 (2004) 1233.
[9] L.T. Canham, Appl. Phys. Lett. 57 (1990) 1046.
[10] A. Puzder, A.J. Williamson, J.C. Grossman, G. Galli, Phys. Rev. Lett. 88 (2002) 097401.
[11] I. Vasiliev, J.R. Chelikowsky, R. Martin, Phys. Rev. B 65 (2002) 121302(R).
[12] F. Iacona, G. Franzo, C. Spinella, J. Appl. Phys. 87 (2000) 1295.
[13] B. Garrido, M. López, A. Pérez-Rodríguez, C. García, P. Pellegrino, R. Ferré, J.A. Moreno, J.R. Morante, C. Bonafos, M. Carrada, A. Claverie, J. de la Torre, A. Souifi, Nucl. Instrum. Methods Phys. Res. B 216 (2004) 213.
[14] M. Luppi, S. Ossicini, Phys. Rev. B 71 (2005) 035340.
[15] G. Hadjisavvas, P.C. Kelires, Phys. Rev. Lett. 93 (2004) 226104.
[16] B. Garrido, M. López, O. González, A. Pérez-Rodríguez, J.R. Morante, C. Bonafos, Appl. Phys. Lett. 77 (2000) 3143.
[17] B. Callas, I. Stenger, C.-C. Kao, S. Fisson, G. Vuye, J. Rivory, Phys. Rev. B 72 (2005) 155319.
[18] G.G. Qin, Y.J. Li, Phys. Rev. B 68 (2003) 85309.
[19] X.X. Wang, J.G. Zhang, L. Ding, B.W. Cheng, W.K. Ge, J.Z. Yu, Q.M. Wang, Phys. Rev. B 72 (2005) 195313.
[20] T.P. Chen, Y. Liu, M.S. Tse, P.F. Ho, D. Gui, S. Fung, Appl. Phys. Lett. 81 (2002) 4724.
[21] T.P. Chen, Y. Liu, M.S. Tse, O.K. Tan, P.F. Ho, K.Y. Liu, D. Gui, A.L.K. Tan, Phys. Rev. B 68 (2003) 153301.
[22] L. Ding, T.P. Chen, Y. Liu, C.Y. Ng, Y.C. Liu, S. Fung, Appl. Phys. Lett. 87 (2005) 121903.
[23] E. Lioudakis, A.G. Nassiopoulou, A. Othonos, Thin Solid Films 496 (2) (2006) 253.
[24] E. Lioudakis, A. Othonos, Opt. Eng. 44 (2) (2005) 023802.
[25] R. Azzam, N. Bashara, Ellipsometry and Polarized Light, North-Holland Publishing, 1977, p. 66.
[26] A.R. Forouhi, I. Bloomer, Phys. Rev. B 38 (1988) 1865.
[27] V. Ioannou-Sougleridis, A.G. Nassiopoulou, A. Travlos, Nanotech 14 (2003) 1174.
[28] Y. Tu, J. Tersoff, Phys. Rev. Lett. 84 (2000) 4393 89 (2002) 086192.
[29] D.R. Hamann, Phys. Rev. B 61 (2000) 9899.
[30] F. Wooten, K. Winer, D. Weaire, Phys. Rev. Lett. 54 (1985) 1392.
[31] D.E. Aspnes, Thin Solid Films 81 (1981) 249.

[32] G.E. Jellison, M.F. Chisholm, S.M. Gorbatkin, Appl. Phys. Lett. 62 (1993) 3348.
[33] R. Hull, Properties of Crystalline Silicon, INSPEC, The Institution of Electrical Engineers, London, UK, 1999.
[34] M. Ben-Chorin, B. Averboukh, D. Kovalev, G. Polisski, F. Koch, Phys. Rev. Lett. 77 (1996) 763.
[35] R. Buczko, S.J. Pennycook, S.T. Pantelides, Phys. Rev. Lett. 84 (2000) 943.
[36] N. Daldosso, M. Luppi, S. Ossicini, E. Degoli, R. Magri, G. Dalba, P. Fornasini, R. Grisenti, F. Rocca, L. Pavesi, S. Boninelli, F. Priolo, C. Spinella, F. Iacona, Phys. Rev. B 68 (2003) 085327.
[37] G. Hadjisavvas, P.C. Kelires, Unpublished.